Research Square

Preprints are preliminary reports that have not undergone peer review.
They should not be considered conclusive, used to inform clinical practice,
or referenced by the media as validated information.

Recycling Aluminium Beverage Cans for Renewable Heating: Design and Evaluation of a Double-Pass Beverage Can Solar Air Heater for Greenhouse Applications

Sishosonke Caspar Nsele

Sonkensele@hotmail.com

University of KwaZulu-Natal

Alaika Kassim

University of KwaZulu-Natal

Sipho Sibanda

Agricultural Research Council of South Africa

Tilahun Seyoum Workneh

University of KwaZulu-Natal

Research Article

Keywords: solar air heaters, discarded aluminium soda cans, temperature difference, instantaneous efficiency, double pass

Posted Date: March 9th, 2026

DOI: https://doi.org/10.21203/rs.3.rs-9044704/v1

License: This work is licensed under a Creative Commons Attribution 4.0 International License.
Read Full License

Additional Declarations: No competing interests reported.

Article Title

Recycling Aluminium Beverage Cans for Renewable Heating: Design and Evaluation of a Double-Pass Beverage Can Solar Air Heater for Greenhouse Applications

Authors and Affiliations

Sishosonke Caspar Nsele (https://orcid.org/0000-0003-3317-726X)[a,b *]
Alaika Kassim (https://orcid.org/0000-0002-3780 -7014) [a],
Sipho Sibanda (https://orcid.org/0000-0002-2971-7078)[b], and
Tilahun Seyoum Workneh (https://orcid.org/0000-0003-3046-2583)[a]

[a] *School of Engineering, University of KwaZulu-Natal, Agricultural Engineering, Pietermaritzburg, KwaZulu-Natal, South Africa*
[b] *Agricultural Research Council, Agricultural Engineering, Gauteng, South Africa*

Corresponding Author

Sishosonke Caspar Nsele - *Sonkensele@hotmail.com*, +27761134449

Acknowledgments

The authors express their gratitude to the University of KwaZulu-Natal and the Agricultural Research Council for facilitating this research.

Abstract

This study evaluated the performance of a low-cost, double-pass beverage can solar air heater (BCSAH) constructed from recycled aluminium beverage cans for potential greenhouse heating, supporting United Nations Sustainable Development Goal 7 (Affordable and Clean Energy). The BCSAH was built with plywood, polystyrene insulation, and a plexiglass cover, incorporating 192 recycled 500 ml cans as the absorber plate. Tests were conducted in Pietermaritzburg, South Africa, under winter conditions at three tilt angles (26°, 31°, 36°) based on photovoltaic winter recommended tilt angles. Key parameters measured included outlet temperature, solar irradiance, thermal efficiency, and heat distribution, using 14 K-type thermocouples, a pyranometer, and an anemometer at a constant air mass flow rate of 0.02 $kg \cdot s^{-1}$. The system achieved significant temperature gains, with second-pass air reaching 128.8°C and maximum outlet temperatures of 94.36 ± 1.35°C. Although tilt angle did not yield statistically significant temperature differences, thermal efficiency increased from 63.36 ± 9.06% for 26° to 67.31 ± 11.78% for 36°. The results highlight the potential of recycled BCSAH to reduce fossil fuel use in greenhouses and other agricultural applications such as soil sterilisation, juice/milk pasteurisation, and pest control. The unit was cost-effective (R 3,470), aligning with circular economy principles and renewable energy goals. Design improvements are suggested, including thinner insulation such as phenolic foam, internal baffles for airflow optimisation, and solar panel integration for off-grid monitoring. Future research should explore multiple units, conduct a broader airflow analysis, and conduct testing across different regions. Integration with heat storage is also recommended.

Keywords: solar air heaters, discarded aluminium soda cans, temperature difference, instantaneous efficiency, double pass

1. Introduction

Renewable energy accounts for only 5.5% of South Africa's total energy supply, with solar thermal contributing just 0.3% [1]. Solar thermal systems are increasingly valued for boosting agricultural productivity and sustainability [2]. They provide heat for crop drying, greenhouse heating, and water heating, reducing fossil fuel use and supporting sustainable practices [3]. The demand for affordable, sustainable heating in greenhouse agriculture is critical for improving yields in cold seasons [4]. Solar air heaters (SAHs), especially those made from recycled materials like aluminium cans, offer a cost-effective and innovative solution [5].

Aluminium production is energy-intensive, accounting for approximately 1% of global GHG emissions and 2.5% of CO_2 emissions, and can take 100–500 years to decompose in landfills [6, 7]. Using cans supports national recycling efforts. This study builds on [4], who promoted sustainable heating for winter greenhouse farming in Pietermaritzburg. However, the focus is on designing, constructing, and evaluating an SAH for potential greenhouse heating. A SAH captures sunlight, converts it to heat, and transfers that heat to the working fluid. Recycled 500 ml aluminium beverage cans can be used as the SAH's absorber plate, turning it into a beverage can solar air heater (BCSAH).

According to literature, terms such as 'soda cans,' 'aluminium cans,' and 'beverage cans' are often used interchangeably. Several researchers have used aluminium cans as absorber plates in SAHs [5, 8-14]. [9] found a 43–55% thermal efficiency at a 38° tilt in Elazığ, Turkey. [10] found 38–68% efficiency at a 24° tilt in Al Kharj, Saudi Arabia. [5] tested aluminium can heaters in Nsukka, Nigeria, achieving up to 65% efficiency and 128°C in a four-pass active system at a 21° tilt. [15] found that increased solar radiation and airflow improved heat absorption and efficiency, while lower flow rates led to higher temperature differences. Higher airflow speeds and better heat transfer between the absorber plate and air significantly improved collector efficiency [15]. Notably, these studies were conducted in Northern Hemisphere countries. In South Africa, the ideal winter tilt angle for PV systems ranges from 26° to 36°, but the optimal angle for solar thermal systems remains unclear [16]. This raises questions about how South Africa's solar radiation intensity would affect BCSAH performance in winter. Lastly, previous studies offer limited construction details. Therefore, this study aims to design, fabricate, and evaluate the performance of a double-pass BCSAH to test in Pietermaritzburg's climatic conditions and offer a detailed breakdown of the heater's construction for replication by farmers.

2. Theoretical design of the beverage can solar air heater

Fig. 1 is a graphical representation of the theoretical SAH. For a glazed SAH, the solar radiation I_c penetrates through the glaze; this reduces the intensity of the solar radiation entering the heater's absorber plate. The product of the transmittance-absorptance factor τα represents the reduction factor. The solar radiation travels and encounters the absorber plate, which then raises the temperature of the absorber plate to T_p. The generated heat then enters the absorber plate, which transfers the heat to the working fluid from the inlet as T_{fi}, and as the working fluid passes through the heater, the temperature increases until it reaches the outlet duct as $T_{fo.}$ Throughout the flow of the working fluid, heat is accumulated as Q_{useful}. The accumulated heat (Q_{useful}) is calculated using the following equations.

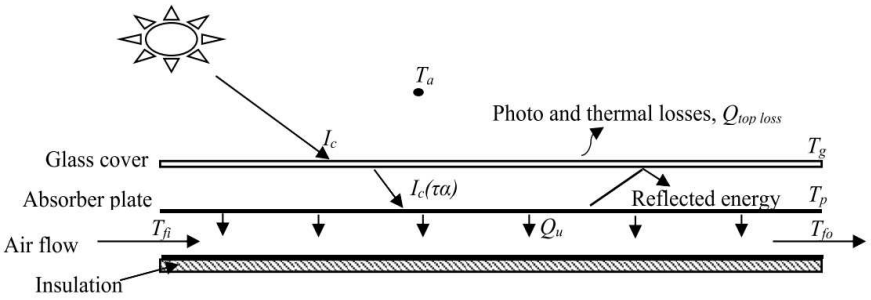


Fig. 1 A schematic diagram of how a SAH collects and converts solar energy to heat [5]

In a steady state, the collector provides useful energy output that is Q_{useful}, equivalent to the rate of radiant energy absorbed by the collector, minus the rate of energy transmitted to its surroundings through the collector's material. The overall useful heat is represented by Equation 1.Where Q_{gain} is the source of heat gain (W), and Q_{loss} is the source of heat loss (W).

$$Q_{useful} = Q_{gain} - Q_{loss} (1)$$

Heat gained by a system is further calculated using the specific heat equation represented by Equations 2 and 3 [5].

$$Q_{useful} = \dot{m} \cdot C_p \cdot (T_o - T_i) (2)$$

$$\dot{m} = \rho \cdot A_o \cdot V_o (3)$$

Where $\dot{m}$ is mass flow rate of the working fluid (dimensionless), C_p is specific heat of air (dimensionless), T_o is outlet temperature (˚C), T_i is inlet temperature (˚C), ρ is density of air ($Kg.m^{-3}$), A_o is area of outlet duct (m^2), andV_o is speed of air at the outlet ($m.s^{-1}$).

The useful heat from the SAH can also be expressed theoretically using the Hottel-Whillier-Bliss equation, expressed in Equation 4 [17].

$$Q_{useful} = A_c \cdot F_R \cdot [I_c(\tau \cdot \alpha) - U_l \cdot (T_i - T_a)] (4)$$

Where Ac is the total collector area (m^2), F_R is heat removal factor (dimensionless), I_c is solar radiation ($W.m^{-2}$),τ is glazing transmittance factor (dimensionless), α is glazing absorptance factor (dimensionless), U_l is solar collector overall heat loss coefficient ($W.m^{-2}.K^{-1}$), T_a is ambient temperature (˚C), and T_i is inlet temperature (˚C) [17].

The heat loss coefficient is the summation of the heat loss coefficients of the collector's top, bottom, and edge surfaces, which determines the collector's overall heat loss coefficient (U_l) represented by Equation 5 [17].

$$U_l = U_t + U_b + U_e (5)$$

Where U_t is the top heat loss coefficient ($W.m^{-2}.K^{-1}$), U_b is the bottom heat loss coefficient ($W.m^{-2}.K^{-1}$), and U_e is the edges heat loss coefficient ($W.m^{-2}.K^{-1}$) [17].

3. Study site and climatic data

Experiments took place at an agricultural research facility in Pietermaritzburg with coordinates 29˚37'39.8'' S, 30˚23'10.6''E " E (Fig. 2) during the 2024 winter season in June and July. Pietermaritzburg experiences dry, sub-humid conditions with an average relative humidity of 52%. The town has an ultraviolet index of 5, with an average temperature of 26 ℃ in January and 19 ℃ in winter. It receives an annual rainfall of 33 mm. Wind speeds vary, with a minimum of 0.30 $km.h^{-1}$ in April, a maximum of 26.60 $km.h^{-1}$ in October, and an average of 8.12 $km.h^{-1}$ throughout the year.

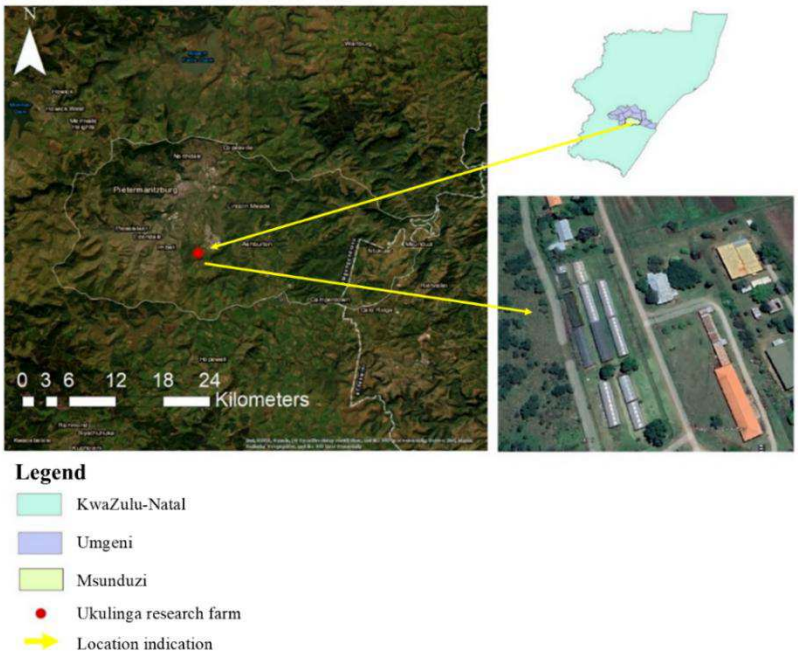


Fig. 2 The experimental site

4. Materials and methods

This section describes the materials used and the methods followed to construct and evaluate the thermal performance of the BCSAH.

4.1 Materials

This section outlines the key materials used to construct the BCSAH and greenhouse system, focusing on low-cost and repurposed components.

4.1.1 Design considerations and specifications

The design considerations for double-pass BCSAH are as follows:

(a) ensure efficient heat transfer with a thermally conductive absorber plate,
(b) maximise heat absorption using high-absorptivity materials,
(c) the absorber surface must be constructed from recycled beverage cans,
(d) design an optimal airflow path with proper spacing and arrangement,
(e) use transparent glazing to reduce heat loss while allowing solar radiation,
(f) select durable, weather-resistant materials for long-term operation,
(g) the BCSAH must harness solar radiation in winter,
(h) the BCSAH must have a double air pass to increase thermal efficiency, and
(i) the BCSAH should have zero to minimum maintenance.

The design specifications of the SAH are:

(a) the bottom of each beverage can must be cut into star-shaped fins to increase heat turbulence [5],
(b) the top of each beverage can must be cut entirely open for connection with the following can [5],
(c) the BCSAH must have an outlet temperature of at least 100 ˚C at noon at time 12h00, and
(d) the heater should have an overall thermal efficiency of at least 61.63% [5].

4.1.2 Beverage can solar air heater prototype design

The BCSAH is a rectangular, box-like structure made from plywood with a thermal resistance of 0.18 $m^2 \cdot K/W$, internally insulated with Polystyrene providing 2.7 $m^2 \cdot K/W$ thermal resistance. It has a clear plexiglass top with

0.85 transmittance and two internal vertical channels separated by a baffle. Each channel is filled with black-painted aluminium cans arranged in columns for double-pass airflow. The total number of cans used is 192 500 ml cans. The collector's dimensions were based on the nighttime heat requirements of the experimental greenhouse, following the methodology of [5]. Fig. 3(a) and (b) show the exploded and collapsed views of the SolidWorks model of the heater design, while Table 1 lists the labelled components. The heater's total weight was calculated as 99 kg, comprising plywood (61.3 kg), plexiglass (29.6 kg), Polystyrene (4.7 kg), and beverage cans (3.4 kg).

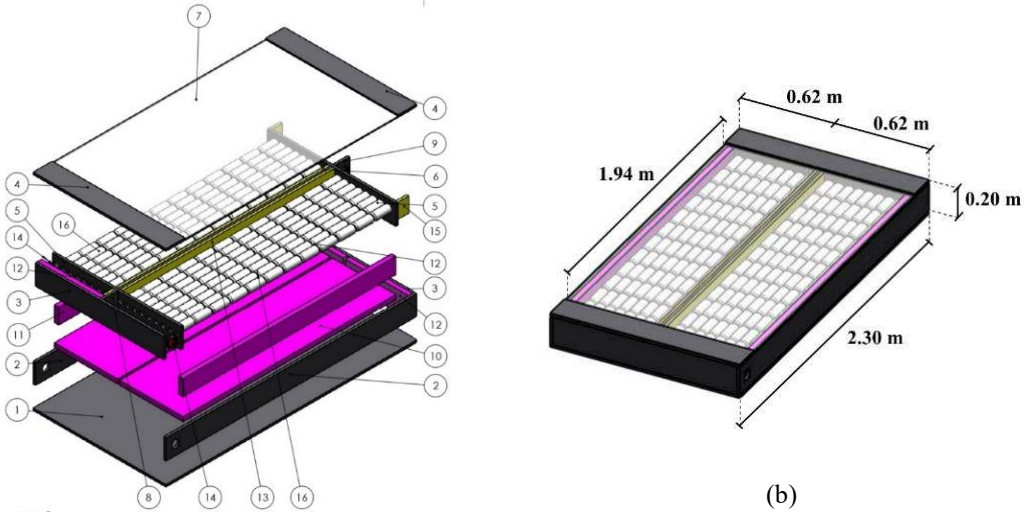


Fig. 3 (a) Exploded and (b) assembled view of the flat plate BCSAH

Table 1 Components of the BCSAH

Part number	Part name
1	Bottom plate
2	Side plate
3	Backplate
4	Fan lid
5	Can holder plate
6	Middle plate
7	Plexiglass cover
8	Section plate
9	Internal fan holder
10	Bottom insulation
11	Side insulation
12	Chamber insulation
13	Middle insulation
14	Extractor fan
15	Small chamber insulation
16	The absorber column can

4.1.3 Beverage can solar air heater construction and assembly procedures

The BCSAH was constructed using 20 mm plywood for both the outer structure and internal components. Plywood was selected for its affordability, low thermal conductivity, ease of handling, and local availability. 20 mm offered the best combination of strength and lightweight. The box was rectangular with two vertical air channels to enable a double-pass airflow system, separated by a wooden baffle. Additionally, 40mm Polystyrene insulation was added to the outside walls and 10mm to the inside walls to retain heat while fitting eight aluminium can absorber tubes, as demonstrated in Fig. 4. A 10 mm plexiglass was used as the glazing material due to its high solar transmittance (0.85) and ease of cutting.

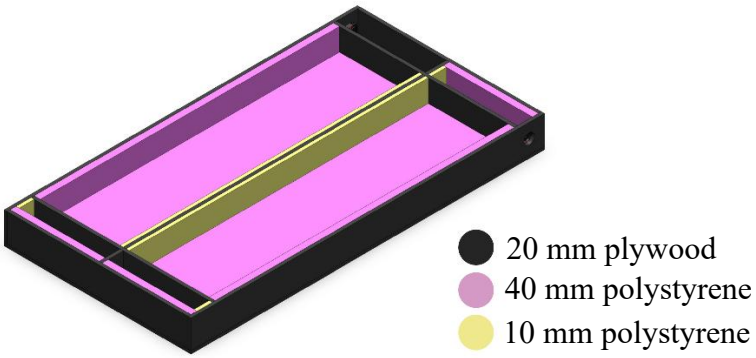


Fig. 4 Locations of the Polystyrene insulation inside the BCSAH

The construction process began by measuring plywood boards using a ruler with an accuracy of ±0.2 cm to match the design specifications for components like the fan lid, insulator plates, and can-support panels. The plywood was then cut to size using a table saw. The plexiglass sheet was trimmed with a hand-held grinder fitted with a 1 mm cutting disc.

Aluminium beverage cans (500 ml) formed the absorber tubes. Each can was opened at the top using a stone grinder, then washed thoroughly with soapy water. The air inlet and outlet holes were marked with a ruler and marker, followed by a star-pattern perforation at the base using a constructed machined cutter, whose dimensions are detailed in Fig. 5.

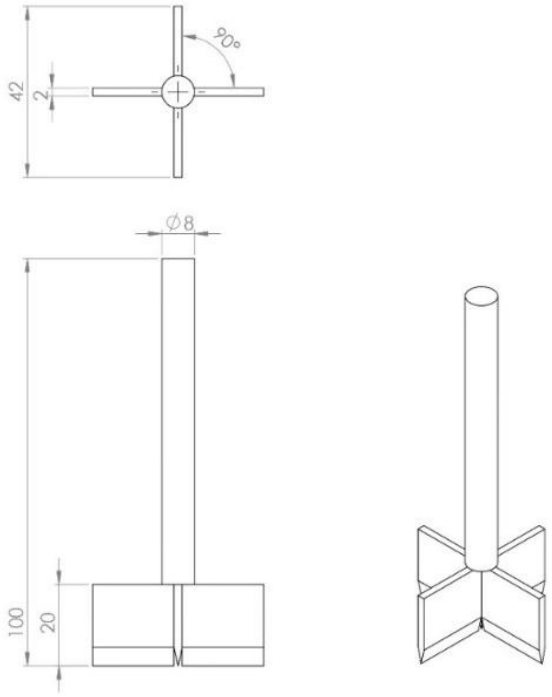
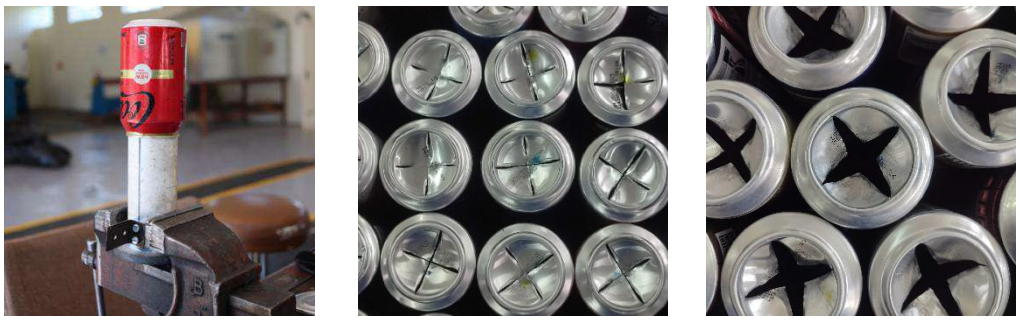


Fig. 5 Engineering drawing of the can cutter, with dimensions in mm

The perforated sections were expanded using a hammer to improve air turbulence, and the backs of the cans were further opened to increase airflow as illustrated in Fig. 6 (a, b and c). The modified cans were glued together into vertical absorber tubes using an 80 Watt Ryobi glue gun and ethylene vinyl acetate glue sticks. Each column contained 12 interconnected cans. Joints were sealed with clear silicone for airtightness. These absorber tubes were arranged vertically into two sets of eight columns, one for each airflow channel, and fastened using ALCOLIN wood adhesive cold glue and ALCOLIN K86 silicone sealant to ensure a sealed interface between cans and supporting plates. The entire absorber structure was painted with Duram NS7 heat-resistant black paint to improve solar absorption. An extractor fan with a mass flow rate of 0.02 $kg \cdot s^{-1}$ was installed at the outlet to drive air through the system. Finally, all components were assembled into the wooden frame to complete the BCSAH.



(a) (b) (c)

Fig. 6 A series of photographs showing the punching back of the can using the a can cutter (a), (b) and (c)

A data logger and perfluoroalkoxy (PFA) insulated K-type thermocouples with a temperature range of -200°C to 260°C (to allow for higher temperature recordings) were installed in the can before the plexiglass enclosed the absorber surface. After the fabrication, the heater was angled, facing the true North and towards the sun for optimal exposure. A dry test of the BCSAH was performed to ensure proper airflow and heating.

4.2 Methods

This section describes the procedures used to test the BCSAH's thermal performance and calculate its efficiency.

4.2.1 Description of the experimental design and procedure

An outdoor experimental setup was developed to perform a performance evaluation off the BCSAH, modifying the methodology of [5]. Experiments took place at an agricultural research facility in Pietermaritzburg. The tests were conducted from the 25th of June to the 19th of July 2024. The SAH faced true North (0˚/360˚) and was tilted at 26˚, 31˚, and 36˚ to determine the optimal angle for performance. These angles align with the recommended range for South African winter conditions (Mukisa and Zamora, 2022). Daily operation began at 06h00, before sunrise (averaging 06h53), and ended at 18h00, after sunset (averaging 17h11). For replication, each tilt angle was tested for five days under clear sky conditions. The weather conditions during the five days for tilt angles of 26º, 31º and 36º are outlined in Table 2. Global solar radiation intensity was measured using a CMP3 Pyranometer (CMP3, Kipp & Zonen, Delft, Netherlands) with a sensitivity of 24–32 $\mu V.W^{-1}.m^{-2}$ at the UKZN agricultural campus weather station. Temperature measurements, including inlet and outlet ducts, were recorded every five minutes across the heater. Fourteen K-type thermocouples (nickel 10% chromium) with a -200°C to 260°C range and ±0.75°C accuracy were installed inside the major air passageways of the cans, as shown in Fig. 7. The K-type thermocouple were calibrated by comparing the readings to the temperature of boiling water at 100°C under the study site standard atmospheric pressure. The thermocouple was immersed until it stabilised, providing a reference point for verifying measurement accuracy.

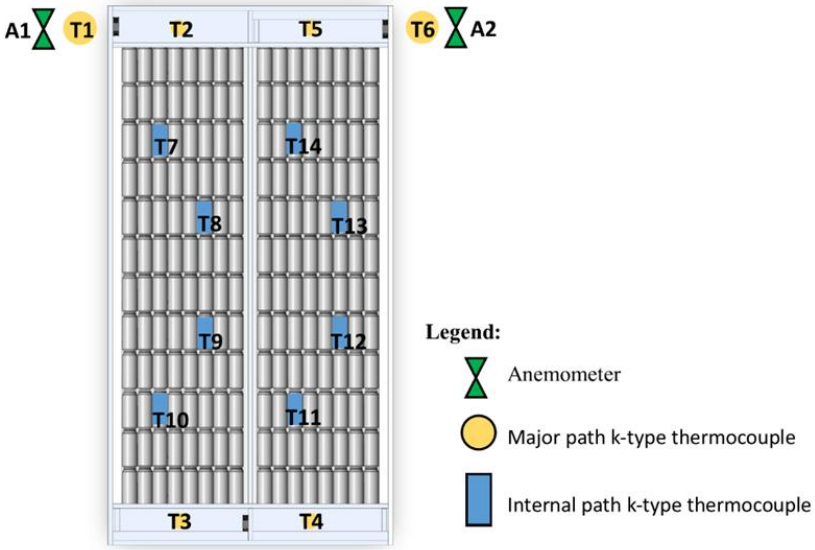


Fig. 7 Locations of the K-type thermocouples at positions T_1 to T_{14} of the BCSAH

In this study, the BCSAH was first evaluated independently under typical winter conditions in Pietermaritzburg. It was then integrated with a greenhouse system, as shown in Fig. 8. The greenhouse was a quonset-shaped structure measuring 8 m × 3 m × 3.5 m, clad with polyethylene film and equipped with 60% shade cloth on the sides to facilitate natural ventilation. A granite-filled sensible heat storage unit was incorporated to store thermal energy from the BCSAH during the day and passively release it into the greenhouse at night.

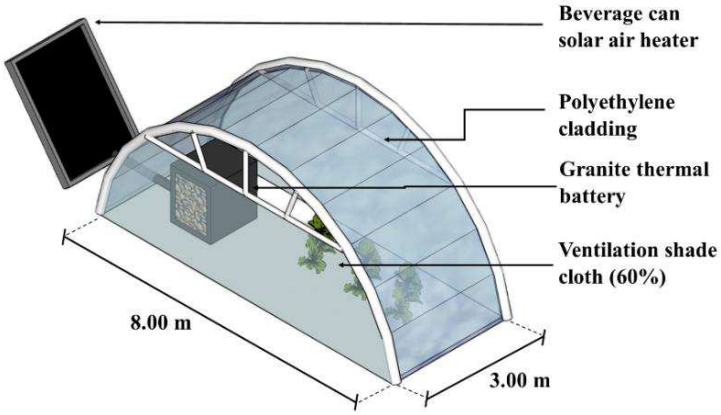


Fig. 8 Phase two experimental set-up of the greenhouse and the BCSAH

Table 2 The weather conditions for each test day at a 26˚ tilt angle

Angle 26					
Parameters	Day 1	Day 2	Day 3	Day 4	Day 5
Date	June 25, 2024	June 26, 2024	June 28, 2024	June 30, 2024	July 19, 2024
Average daily temperature(˚C)	12.4	13.3	14.2	15.1	17.2
Sunshine hours(minutes)	615	616	616	617	629
Sunrise time	06h53	06h53	06h53	06h53	06h50
Sunset time	17h08	17h09	17h09	17h10	17h19
Angle 31					
Parameters	Day 1	Day 2	Day 3	Day 4	Day 5
Date	July 01, 2024	July 05, 2024	July 06, 2024	July 17, 2024	July 18, 2024
Average daily temperature(˚C)	16.1	13.3	11	12.6	13.6
Sunshine hours(minutes)	617	619	620	628	629
Sunrise time	06h53	06h53	06h53	06h50	06h50
Sunset time	17h10	17h12	17h13	17h18	17h19
Angle 36					
Parameters	Day 1	Day 2	Day 3	Day 4	Day 5
Date	July 12, 2024	July 13, 2024	July 14, 2024	July 15, 2024	July 16, 2024
Average daily temperature(˚C)	18.9	17.6	14.4	15.3	14.2
Sunshine hours(minutes)	623	624	626	626	627
Sunrise time	06h52	06h52	06h51	06h51	06h51
Sunset time	17h15	17h16	17h17	17h17	17h18

4.2.2 Description of data collection and instrumentation

Temperature data was recorded using a digital PC-Logger DataTaker DT82I Series 4 digital recorder, featuring five measuring channels and paired with 14 fixed K-type thermocouples. The associated computer program, the dEX program, facilitates integration with the recording process. The data recorder's output was retrieved at predefined intervals of 5 minutes and subsequently archived in the hard drive of a personal computer. Air mass flow rate measurements were conducted using an RS PRO AVM-01 vane anemometer placed at the fan opening duct with a diameter of 70mm to assess the outward air velocity. Subsequently, the acquired air velocity data underwent multiplication by the cross-sectional area of the air blower and air density. Fig. 9 illustrates the experimental design.

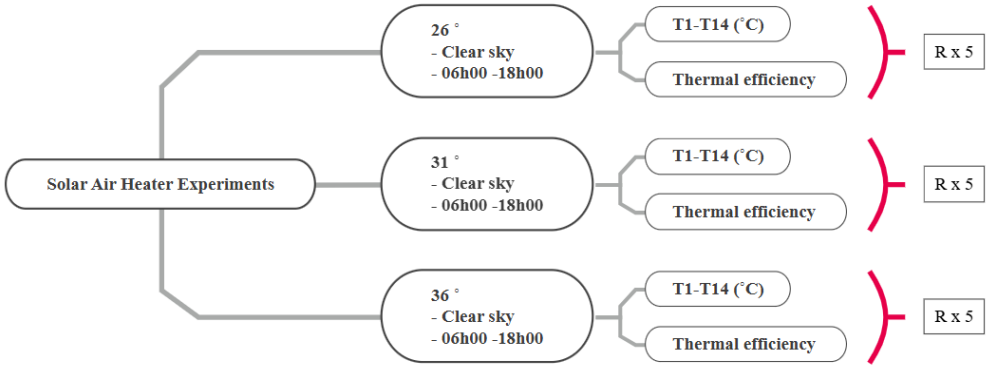


Fig. 9 The breakdown of the experimental procedure

4.3 Data analysis

This section presents theoretical and statistical data analysis of the BCSAH.

4.3.1 Theoretical analysis

Both instantaneous and overall thermal efficiencies were calculated to evaluate the thermal performance of the BCSAH. The mass flow rate of air was determined using Equation 6, where ρ is the density of air ($Kg.m^{-3}$), A_o is the area of the fan opening (m^2), and V_o is the linear flow velocity of air ($m.s^{-1}$).

$$\dot{m} = \rho A_o V_o (6)$$

The useful thermal energy output was then calculated using Equation 7, where c_p is the specific heat capacity of air, and T_1 and T_6 are the inlet and outlet air temperatures, respectively.

$$Q_u = \dot{m} c_p (T_1 - T_6) (7)$$

Instantaneous thermal efficiency was calculated using Equation 7, where A_c is the area of the collector's absorber plate (m^2), I_c is the solar irradiance ($W.m^{-2}$) on the collector surface at each time step. Finally, the overall daily thermal efficiency was obtained by integrating both the useful energy output and the solar input over the daylight period (sunrise to sunset), using Equation 8 and Equation 9. These calculations collectively enabled a comprehensive assessment of the system's thermal efficiency throughout the day.

$$\eta_{inst} = \frac{Q_u}{A_c I_c} (8)$$

$$\eta_{overall} = \frac{\int_{sunset}^{sunrise} Q_u dt}{\int_{sunset}^{sunrise} A_c I_c dt} \times 100 (9)$$

4.3.2 Statistical analysis

Descriptive statistics were used to characterise the diurnal performance of the BCSAH. A one-way ANOVA was performed to assess the effect of tilt angle (26°, 31°, and 36°) on outlet temperature (T_6) and on the overall efficiency. If significant differences were found ($p < 0.05$), Tukey's HSD post hoc test was applied to identify which angles differed [18].

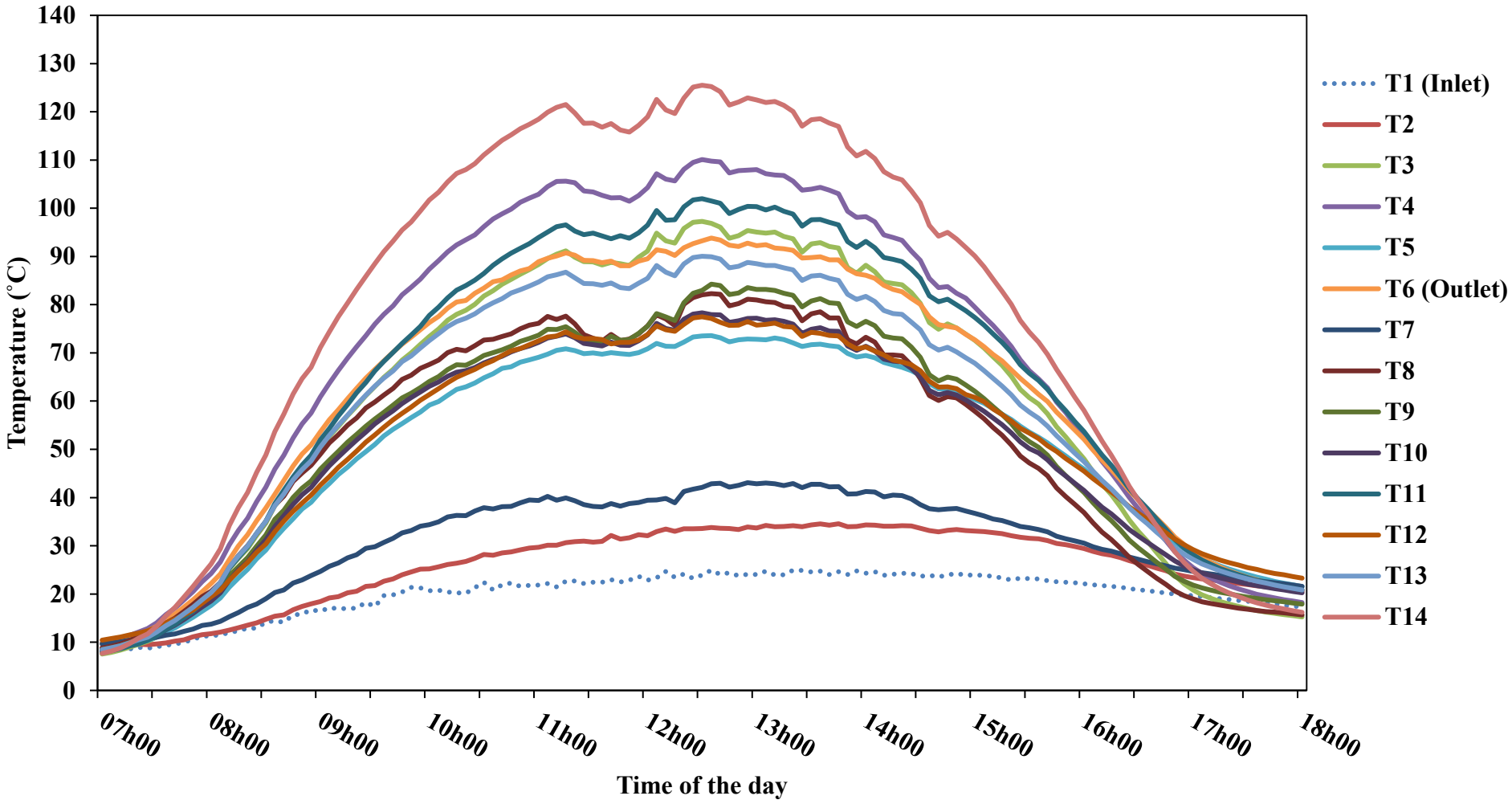
5. Results and discussion

This section presents and discusses the key findings from the evaluation of the BCSAH.

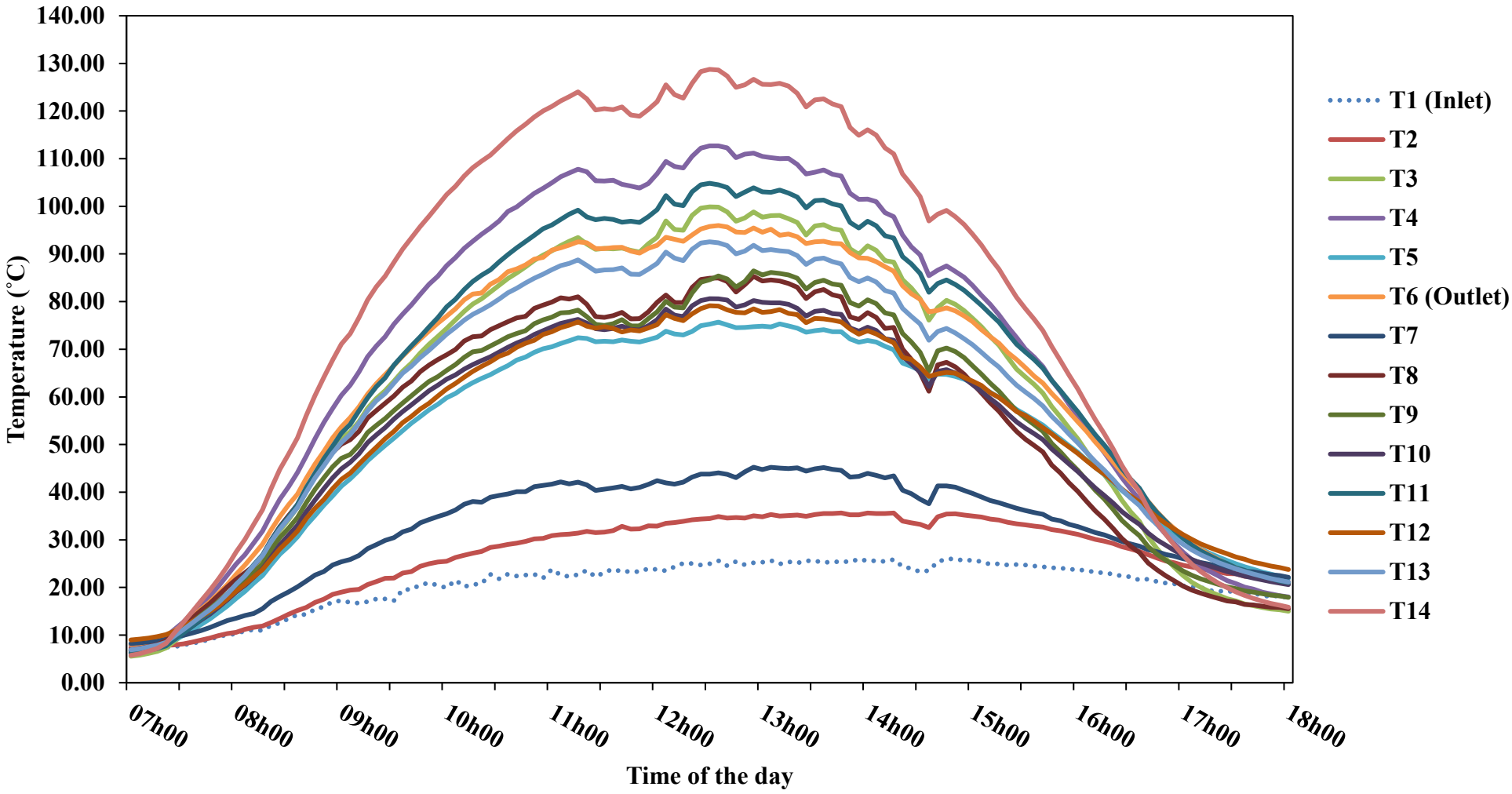
5.1 Diurnal and time series analysis at 26°, 31°, and 36° tilt angle

Fig. 10 to Fig. 12 show the BCSAH's internal temperature distribution at the locations highlighted in Fig. 7 for tilt angles of 26°, 31°, and 36°. The beverage can absorber plate raised air temperatures above ambient at all points, with temperatures rising in the morning, peaking around 12h30, and declining in the evening, as also reported by [5].

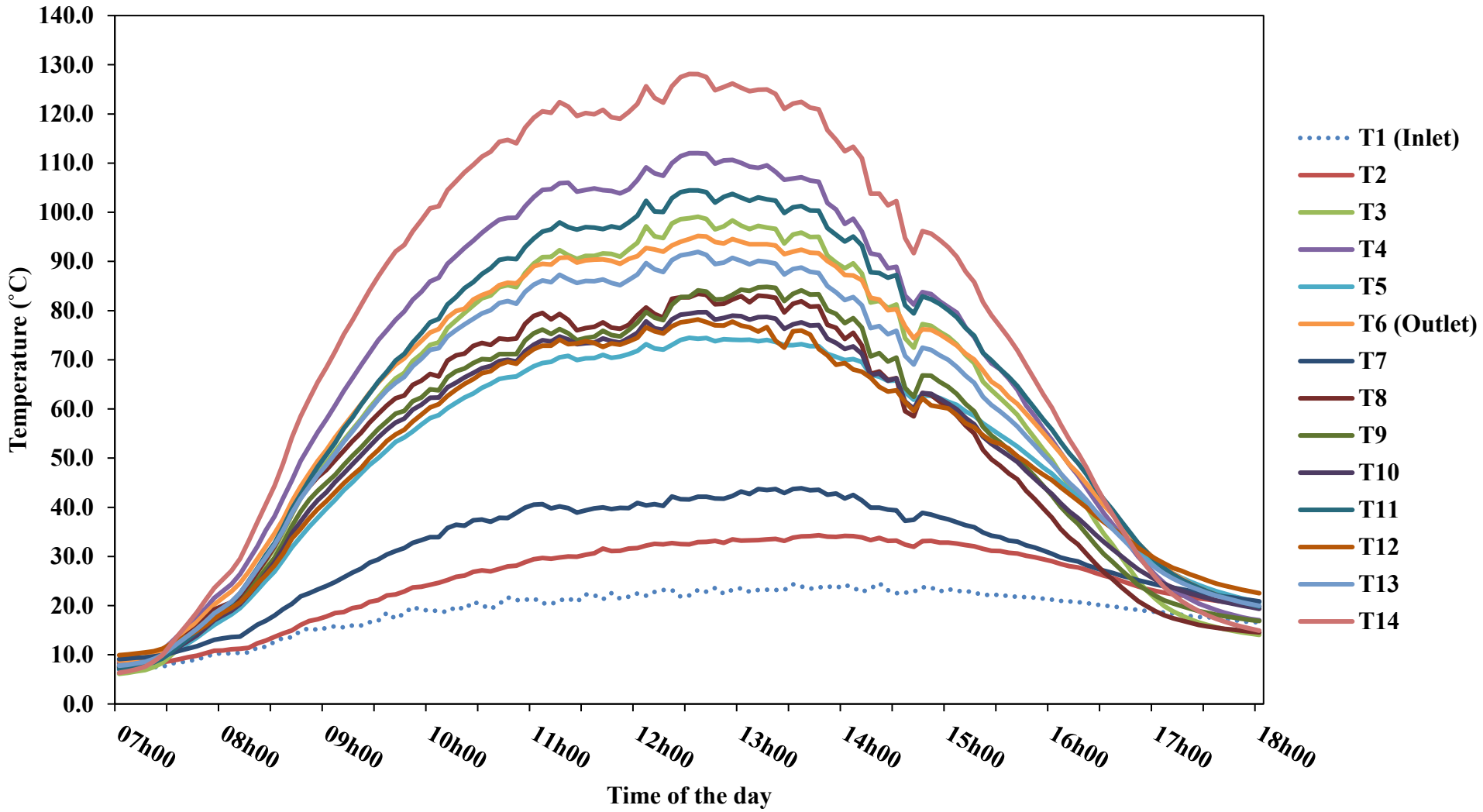
The highest temperature was recorded at T_{14}, with mean values of 122.55 ± 2.20 °C (CV = 1.80%) at 26°, 125.81 ± 2.27 °C (CV = 1.80%) at 31°, and 125.55 ± 2.12 °C (CV = 1.69%) at 36°, with low CVs (<2%) indicating highly consistent thermal performance at T_{14} for all tilt angles. This stability at peak temperatures demonstrates reliable heat capture by the BCSAH under Pietermaritzburg winter conditions. The 31° tilt produced the highest instantaneous peak of 128.08 °C at 12h00. While [5] reported 128 °C at the outlet, T_{14} in this study T_{14} is an internal point in channel two just before the outlet. Nevertheless, it reflects the system's peak temperature elevation.



289
290 **Fig. 10** Temperature profile of the BCSAH over time at 26°
291



292
293 **Fig. 11** Temperature profile of the BCSAH over time at 31°



294
295 **Fig. 12** Temperature profile of the BCSAH over time at 36°

5.2 Diurnal and time series analysis at 26°, 31°, and 36° tilt angle focusing on the inlet and outlet

Solar irradiance throughout the day influences the rise in the internal and outlet temperatures, as illustrated in Fig. 13 to Fig. 15, which highlight the T_6 relative to T_1 and solar irradiance for tilt angles of 26°, 31°, and 36°, while Fig. 16 provides a side-by-side comparison of T_6 across these angles. T_6 displayed a consistent diurnal pattern, rising steadily in the morning, peaking around 12h30, and declining in the evening, closely following the daily solar irradiance profile. Solar intensity rises with solar elevation, peaking at noon as the sun's rays become most direct and the atmospheric path length shortest [21]. Peak mean outlet temperatures were 92.02 ± 1.30°C (CV = 1.41%) at 26°, 94.36 ± 1.35°C (CV = 1.43%) at 31°, and 93.54 ± 1.27°C (CV = 1.36%) at 36°, indicating high consistency across tilt angles, with the highest occurring at 31° around 12h35. Minor dips in temperature between 11h00 and 12h00 at 26° and 31° were attributed to transient cloud cover. Solar intensity decreases with cloud cover because clouds block and scatter direct sunlight, increasing diffuse solar irradiance while reducing the total irradiance that reaches the surface [22].

Comparisons with other studies highlight the role of geographic and climatic factors in SAH performance. [12] reported a peak temperature of 66 °C in summer using external reflectors, while [23] recorded 51.5 °C in a finned double-pass heater during winter in Iraq. Higher temperatures were achieved by [5] in Nigeria, reaching 101.2 °C with passive airflow and 128 °C with active airflow, whereas [14] observed lower values (32.8–36.2°C) in unglazed vertical designs in Turkey. Latitude is particularly influential, with regions closer to the equator, such as Nigeria (≈620 km from the equator), generally recording higher temperatures than more distant locations, such as Turkey (≈4140 km).

A one-way ANOVA showed no significant differences in T_6 across the tested tilt angles ($p > 0.05$), indicating statistically similar temperature outputs within this range. This finding aligns with the tilt angles typically recommended for PV systems, suggesting that the same range can be effectively applied for BCSAH winter installations in South Africa [16].

In contrast, time of day significantly influenced heat gain ($p < 0.05$), with peak values between 11h00 and 13h00 at T6 and T14, coinciding with maximum solar irradiance. This indicates that farmers can plan activities requiring higher temperatures within this window to optimise energy use. These results align with solar thermal principles, as greater irradiance drives higher heat absorption. The BCSAH's ability to exceed 94 °C highlights its effectiveness in converting solar energy into usable heat. Consistently high and predictable temperatures make it suitable for applications such as pasteurisation, pest control, accelerated composting, and integration into hot-water systems [19, 20]. Its reliable output, directly linked to solar irradiance and time of day, enables effective scheduling while reducing fossil fuel dependence, thereby enhancing energy efficiency and environmental sustainability.

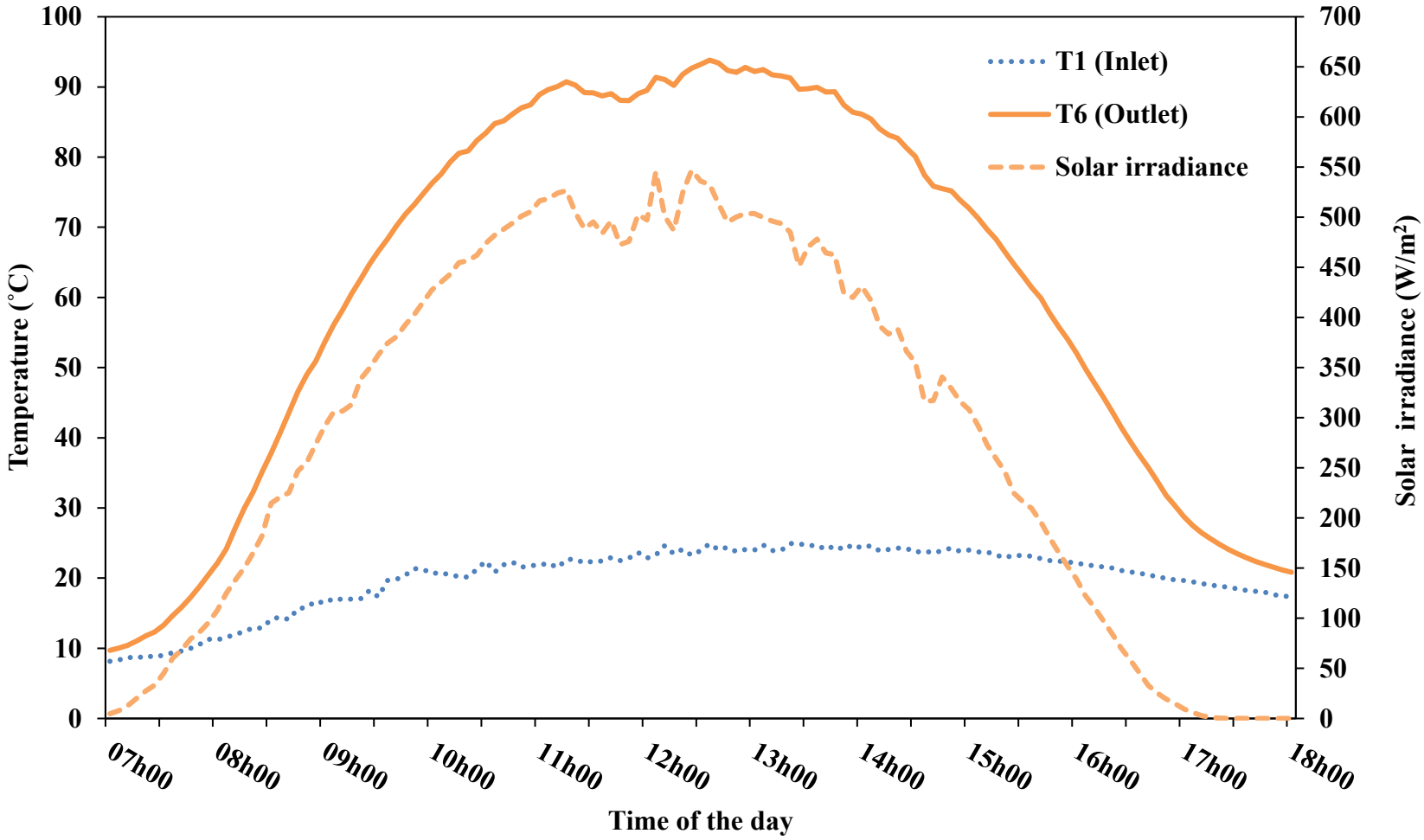
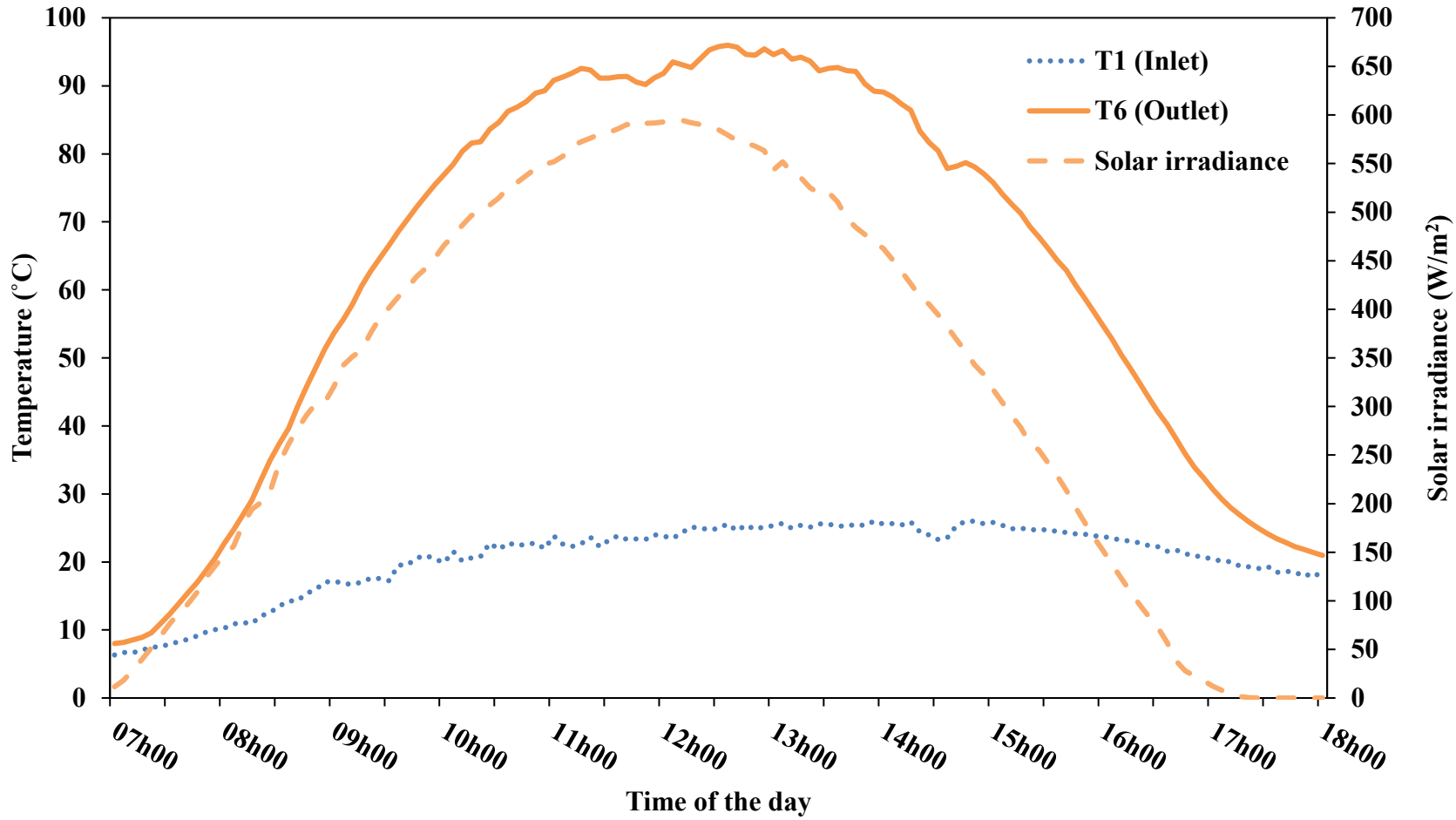


Fig. 13 Variation of temperature and solar irradiance versus time of the day at an angle 26°



334
335 **Fig. 14** Variation of temperature and solar irradiance versus time of the day at angle 31°

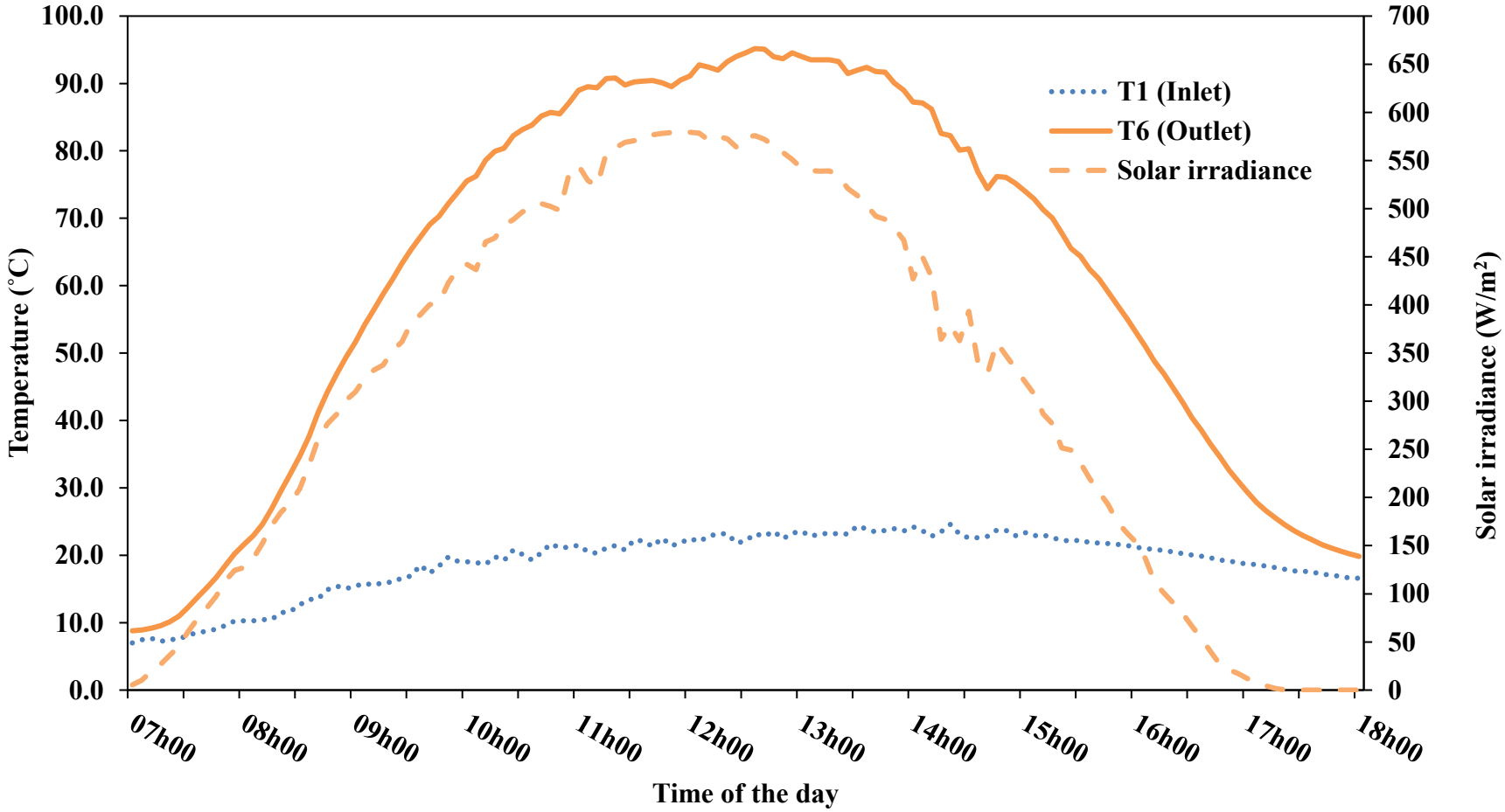
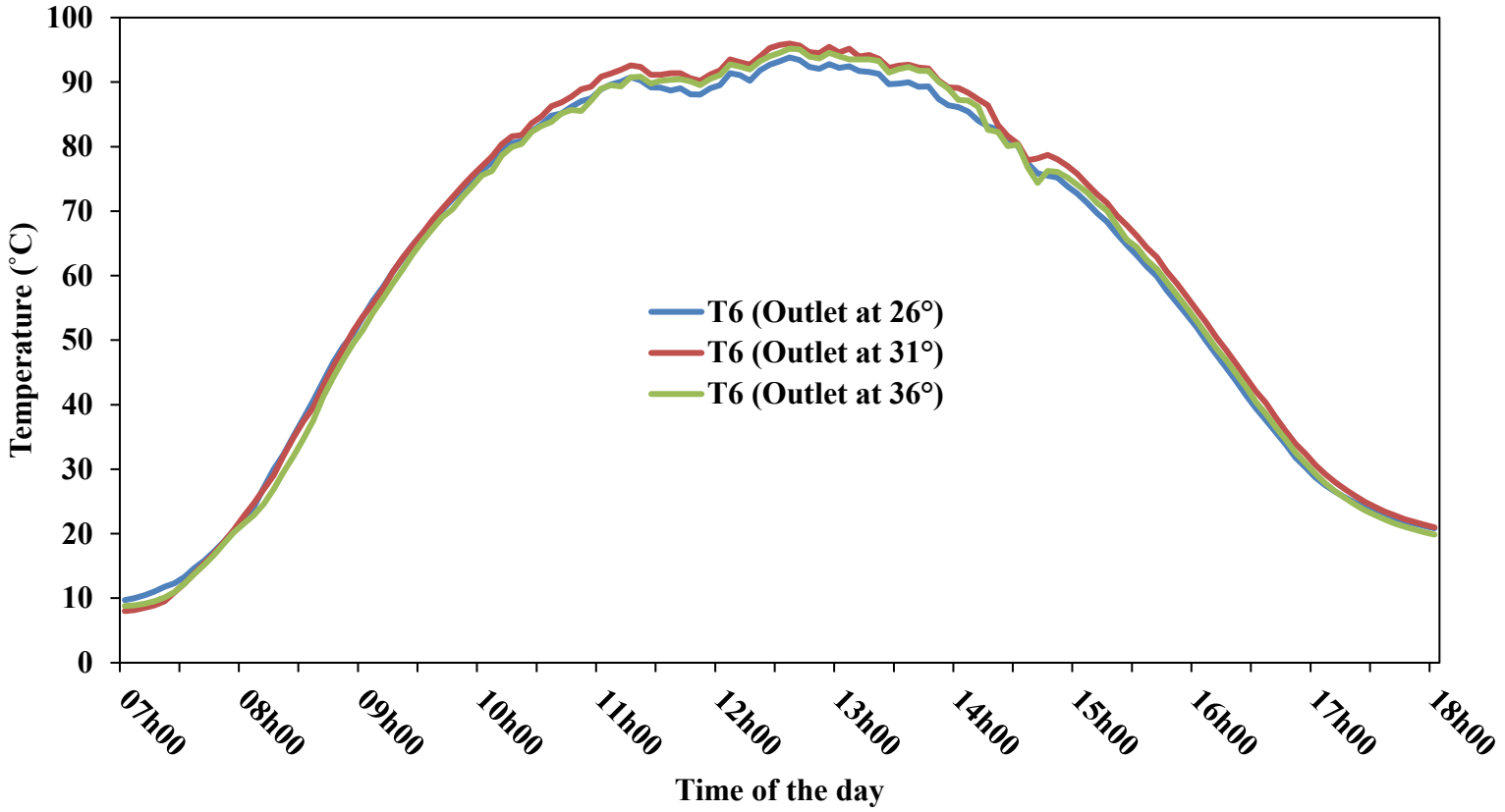


Fig. 15 Variation of temperature and solar irradiance versus time of the day at an angle of 36°



338
339 **Fig. 16** Side by side comparison of the outlet temperature at angles 26 °, 31 °, and 36 °

5.3 Relationship between solar irradiance and outlet temperature of bcsah

The study observed a linear relationship between solar irradiance and outlet T_6 in the BCSAH, illustrated in Fig. 17 to Fig. 19. The temperature differences between T_6 and T_1 followed the same trend as irradiance increased from sunrise to midday and declined thereafter. A Pearson correlation analysis confirmed this with a strong positive correlation across all three tilt angles tested highlighted in Table 3.

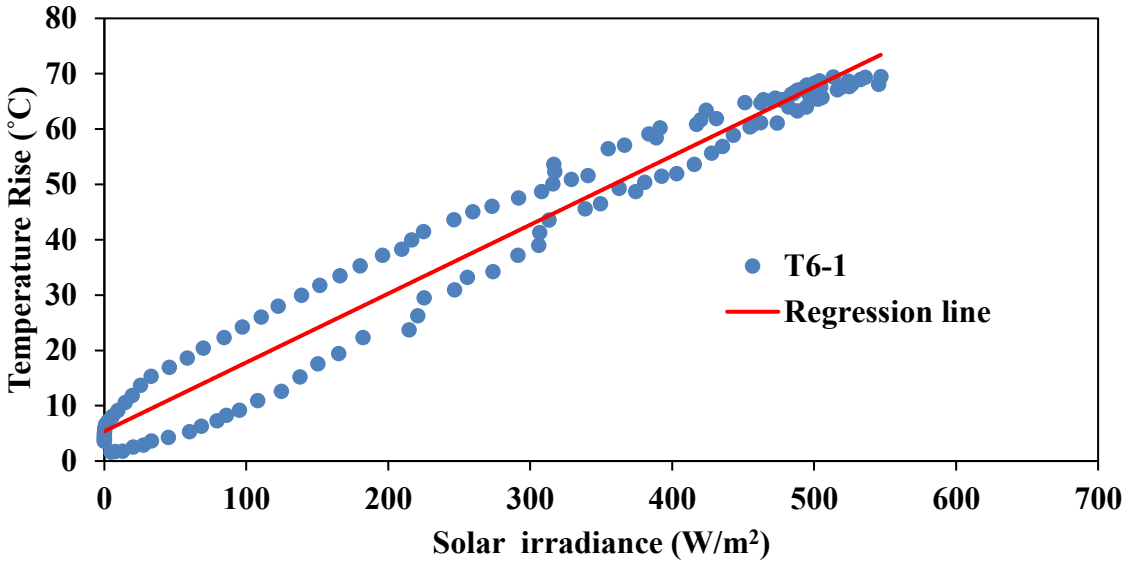


Fig. 17 Variation of temperature difference with solar irradiance at angle 26°

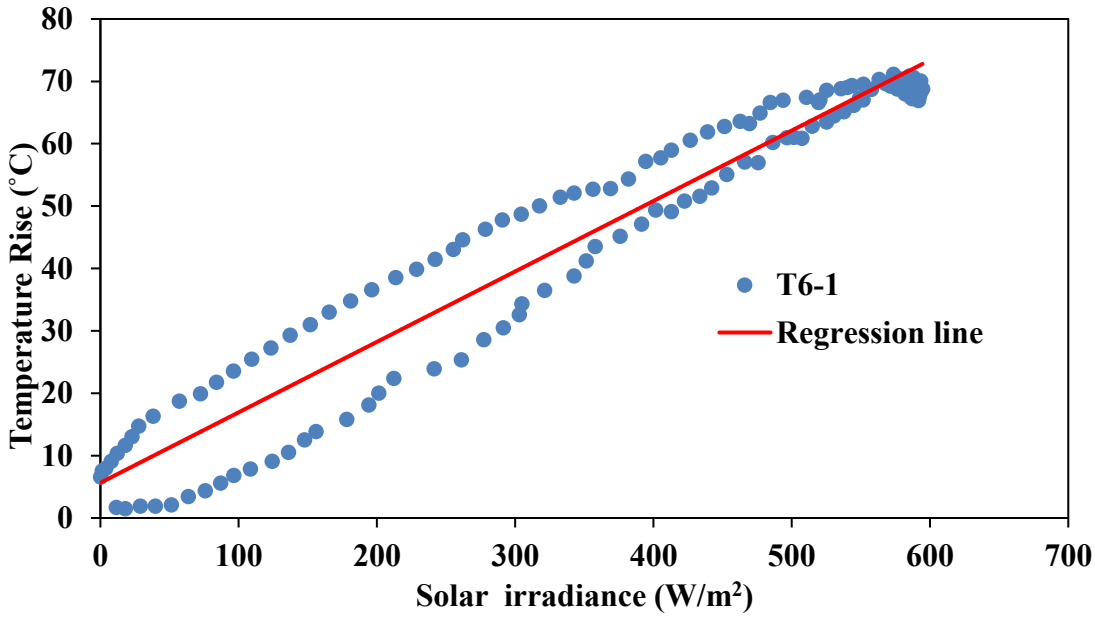


Fig. 18 Variation of temperature difference with solar irradiance at angle 31°

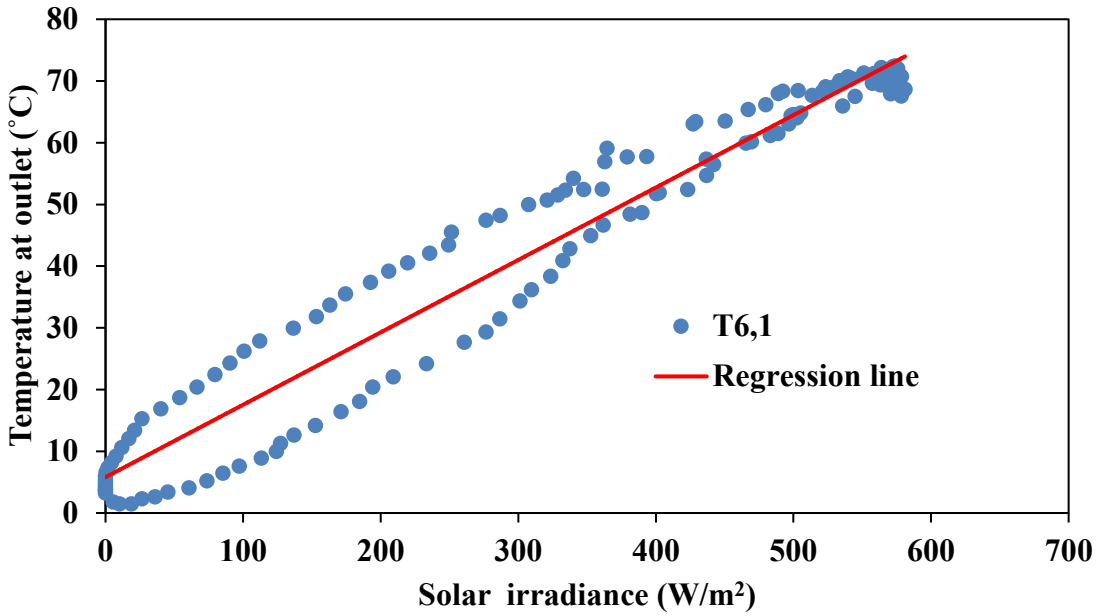


Fig. 19 Variation of temperature difference with solar irradiance at angle 36˚

This relationship is thermodynamically expected and empirically validated [5, 14]. Higher solar irradiance delivers more energy to the absorber plate, increasing air heating and outlet temperature, while reduced irradiance lowers the heat transfer rate. Such behaviour is well-documented in SAH research, where outlet temperatures consistently peak near noon in tandem with maximum radiation intensity [5, 8-14].

The findings reinforce this established principle while confirming that a double-pass BCSAH constructed from recycled aluminium cans under South African winter conditions. This adds contextual evidence that performance remains tightly coupled to solar availability.

Table 3 Correlation analysis of isolation and outlet air temperature at tilt angles of 26°, 31°, and 36°

Tilt angle	r (Pearson Correlation)	p-value	n
26°	0.957	< 0.001	132
31°	0.935	< 0.001	132
36°	0.944	< 0.001	132

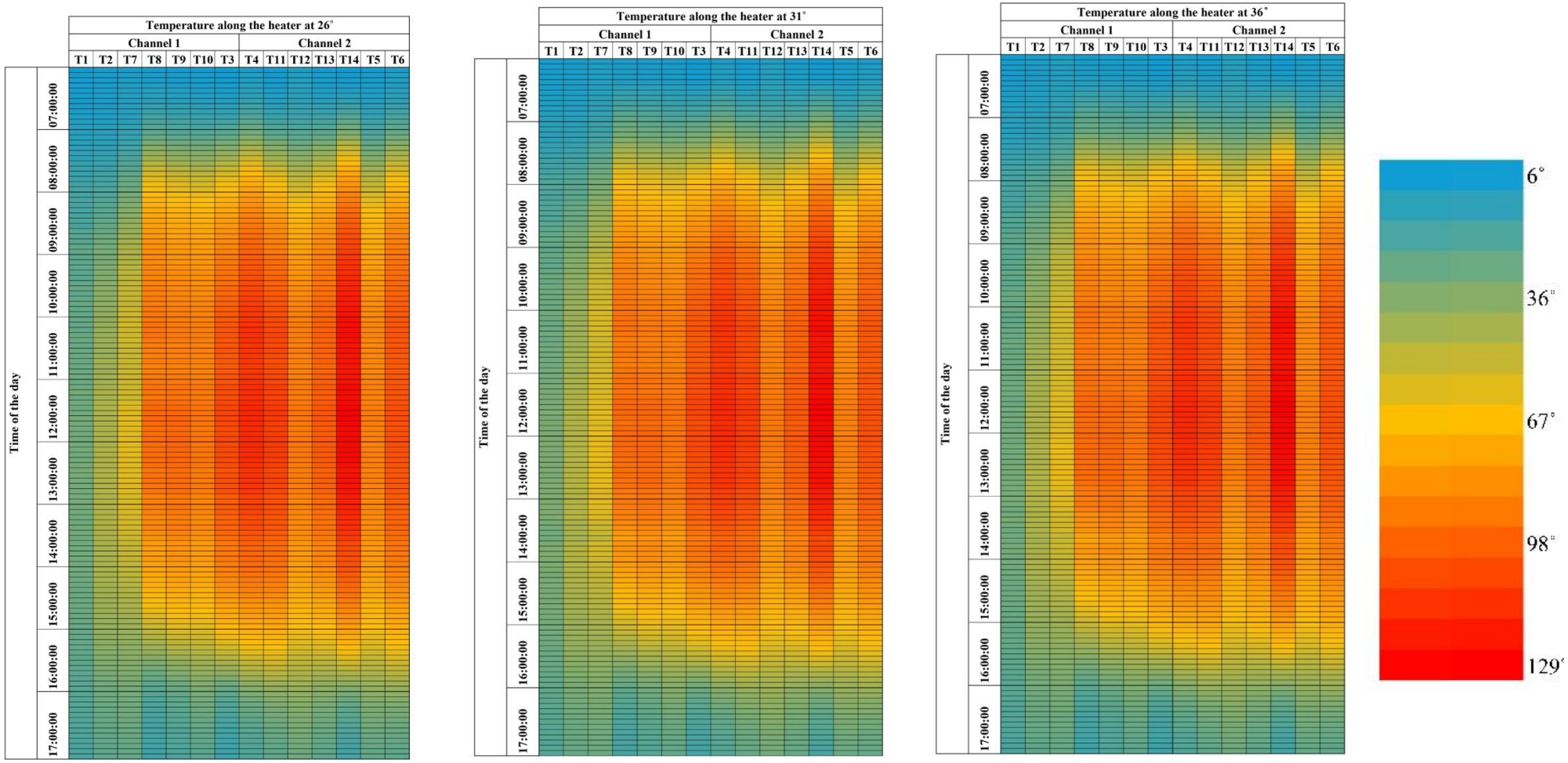
5.4 Observed versus the expected temperature profiles in the bcsah

The BCSAH was expected to exhibit a progressive temperature rise from T1 to T6 following the sequence: $(T_1 \approx T_2) < T_7 < T_8 < T_9 < T_{10} < (T_3 \approx T_4) < T_{11} < T_{12} < T_{14} < (T_5 \approx T_6)$, with similar readings at $T_1 \approx T_2$, $T_3 \approx T_4$, and $T_5 \approx T_6$ due to the absence of absorber material. However, heat maps in Fig. 20 revealed deviations from this pattern. In Channel One (T_1–T_3), temperatures generally increased throughout the day, with a slight drop at T9. In Channel Two (T_4–T_6), temperatures declined, indicating ineffective heat gain and potential losses. The observed sequence was: $T_1 < T_2 < T_7 < T_5 < T_{12} < T_{10} < T_9 < T_8 < T_{13} < T_6 < T_3 < T_{11} < T_4 < T_{14}$, suggesting uneven heat distribution influenced by airflow and localised losses. These temperature drops identify areas requiring further investigation to enhance heat retention.

Suboptimal airflow patterns and localised heat losses likely contribute to the uneven temperature distribution. The temperature declines in Channel Two, indicating areas where heat is not effectively absorbed or is lost to the surroundings instead of being transferred to the working fluid. Identifying these unexpected drops provides critical

379 insights for improving the system's design. Addressing such inefficiencies could yield higher and more consistent
380 outlet temperatures, enhancing the BCSAH's suitability for agricultural applications that require sustained heat.

381



(a) (b) (c)

382 **Fig. 20** Heat maps of the working fluid throughout the BCSAH, from the inlet to the outlet at a tilt angles of (a) 26˚, (b) 31˚ and (c) 36˚

5.5 Thermal efficiency

Fig. 21 shows how the instantaneous thermal efficiency of the BCSAH varies with tilt angle throughout the day. Efficiency was calculated using the temperature difference between T_6 and T_1, representing total thermal efficiency from both channels. Efficiency rose sharply in the morning, stabilised at 60–65% between 10h00 and 14h00, and increased again in the late afternoon due to thermal lag, when retained heat sustained high T_6 temperatures relative to the decreasing T_1, thus increasing the T_6–T_1 differences. Among the three tilt angles tested, 36° consistently produced the highest efficiencies, particularly in the afternoon, followed by 31° and 26°. Mean efficiencies increased slightly with tilt angle, with 63.36 ± 9.06% (CV= 14.40%) for 26°, 64.69 ± 11.12% (CV= 17.19%) for 31°, and 67.31 ± 11.78% (CV= 17.50%) for 36°. The moderate CV values (14–18%) reflect greater variability in efficiency compared to peak temperatures, suggesting that external factors such as cloud cover and internal heat losses introduced fluctuations, even though overall trends with tilt remained consistent.

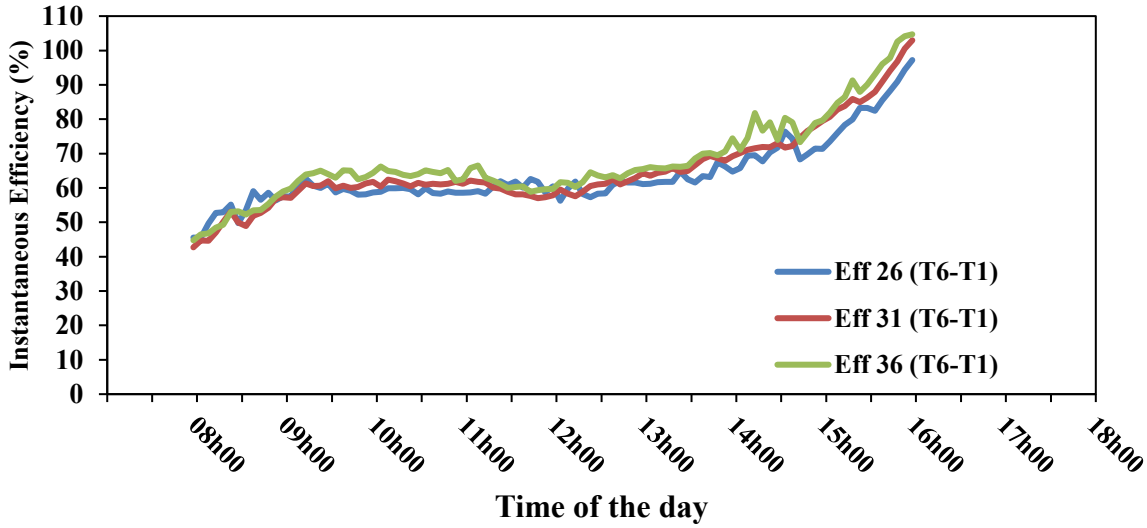


Fig. 21 Instantaneous efficiency (T_6–T_1) of the BCSAH at different tilt angles

External and internal factors likely influenced efficiency results. Cloud cover between 11h00 and 12h00 (noted at 26° and 31°) introduced variability, lowering instantaneous efficiency values. Internally, the heater exhibited uneven temperature progression as highlighted in sections 5.1.1 and 5.1.4, indicating localised heat losses.

The efficiencies achieved align with those reported for other can-based SAHs. [9] reported 55%, [5] achieved 65%, and [14] reached a maximum of 76.22% in unglazed vertical can-fin systems. These comparisons confirm that a BCSAH built from recycled materials can perform competitively with established designs.

A one-way ANOVA revealed no statistically significant differences in efficiency among tilt angles ($p > 0.05$), consistent with the lack of significant tilt effects on T_6 temperatures. Thus, within 26°–36°, tilt angle minimally influences efficiency under Pietermaritzburg winter conditions. This finding is valuable in practice, since it suggests that solar thermal systems can adopt the same tilt range used for PV systems, simplifying installation.

5.6 Cost estimation

The construction of the BCSAH, with a collector area of 3.2 m², incurred a total cost of R 3,470, translating to an approximate unit cost of R 1,084.38 per square meter (m²). The primary material expenses came from the plexiglass, plywood, and polystyrene insulation, as highlighted in Table 4. Comparing these findings with other studies, the BCSAH's cost efficiency is noteworthy. [12] indicated that SAHs have lower production, operating, and maintenance costs without providing specific figures. [11] Reported a construction cost of US$60 for a smaller 0.6 m² heater and cabinet dryer. When converted and scaled, this equates to approximately R 1,065.65/m². The present study's BCSAH, achieved similar cost efficiency but at a larger scale.

Table 4 Approximate estimation of the BCSAH construction cost in ZAR

Item No.	Description	Unit	Quantity	Total Price (ZAR)
1	20 mm Plywood sheets	m²	3.2	650
2	40 mm Polystyrene insulation	m²	3.2	520
3	10 mm Polystyrene insulation	m²	2	95
4	10 mm Plexiglass	m²	2.4	1100
5	500 ml Aluminium beverage cans	cans	192	-
6	Wood glue	Litre	1	100
7	EVA glue sticks (for glue gun)	pcs	1	160
8	Clear silicone sealant	Cartridge	2	170
9	Black heat-resistant paint	Litre	1	290
10	Extractor fan (0.02 kg/s)	Unit	3	360
12	Screws, No.8, 4mm x 60mm	50 pieces	1	25
	Total			3470

6. Conclusions

This study designed, built, and tested a standalone double-pass BCSAH using recycled aluminium cans to provide sustainable, low-cost greenhouse heating in support of food security and the UN SDGs (2030). Experiments took place at an agricultural research facility in Pietermaritzburg, under typical winter conditions of the location, assessing three tilt angles: 26°, 31°, and 36° based on photovoltaic tilt recommendations for optimal winter performance. The BCSAH consistently raised internal air temperatures above ambient and exhibited a strong positive correlation between solar irradiance and outlet temperature, particularly at 26° ($r = 0.957$, $p < 0.001$). Temperature patterns closely mirrored solar radiation, peaking around 12h30. Maximum internal temperatures reached 128.8°C at T_{14}, while average peak outlet temperatures (T_6) ranged from 92.02°C to 94.36°C, demonstrating suitability for agricultural and domestic heating. Time of day significantly influenced heat gain ($p < 0.05$), with the period between 11h00 and 13h00 identified as optimal. Although efficiency tended to increase with tilt angle, differences were not statistically significant, indicating that in South Africa, solar thermal systems perform optimally at the same tilt angles as photovoltaic systems.

Analysis of internal temperature profiles revealed uneven heat distribution and unexpected drops, particularly in Channel Two, deviating from the theoretically expected progressive temperature rise. This highlights opportunities to optimise internal design, enhance heat retention, and improve transfer efficiency. Constructed from plywood, plexiglass, insulation, silicone, and recycled cans, the BCSAH demonstrated cost-effectiveness and alignment with circular economy principles. It efficiently captured solar energy, delivered substantial temperature gains, and identified optimal operating angles under local conditions, affirming its potential as a sustainable greenhouse heating solution that reduces reliance on fossil fuels.

7. Recommendations for future research

The design recommendations for future research should focus on identifying key temperature drop zones to pinpoint causes of ineffective heat gain and localised losses, and evaluating the necessity of the second pass given observed declines in Channel Two, including comparisons with single-pass or modified multi-pass designs supported by additional airflow measurements to capture internal heat distribution more comprehensively. Enhancing resilience to transient cloud cover or short-term solar irradiance fluctuations through heat storage integration or adaptive control mechanisms is recommended, alongside optimising internal airflow and improving insulation using thinner, high-performance materials such as phenolic foam to achieve higher and more consistent

outlet temperatures. Additional improvements include adding thermal mass, sealing leaks, installing windbreaks, and incorporating solar panels for off-grid operation and system monitoring.

Methodology recommendations include constructing at least three BCSAH units for parallel testing under identical conditions for a reliable comparison. The system should also be tested at tilt angles beyond the 26–36 °C range. More airflow anemometers should be positioned within the heater, not only at the sides, to better capture internal airflow dynamics. Testing in diverse South African geographic locations is essential to evaluate the system's robustness and applicability. Finally, future studies should assess key temperature drop zones to determine whether the second pass is necessary.

8. References

1. Akinbami, O.M., Oke, S.R. and Bodunrin, M.O. (2021). The state of renewable energy development in South Africa: An overview. *Alexandria Engineering Journal* 60 (6): 5077-5093. https://doi.org/10.1016/j.aej.2021.03.065
2. Olabi, A.G., Shehata, N., Maghrabie, H.M., Heikal, L.A., Abdelkareem, M.A., Rahman, S.M.A., Shah, S.K. and Sayed, ET. (2022). Progress in solar thermal systems and their role in achieving the sustainable development goals. Energies 15 (24): 9501. https://doi.org/10.3390/en15249501
3. Hassanien, R.H.E., Li, M. and Lin, .WD. (2016). Advanced applications of solar energy in agricultural greenhouses. *Renewable and Sustainable Energy Reviews* 54 989-1001. https://doi.org/10.1016/j.rser.2015.10.095
4. Thipe, E.L., Workneh, T., Odindo, A. and Laing, M.. (2017). Greenhouse technology for agriculture under arid conditions. *Sustainable Agriculture Reviews* 37-55. https://doi.org/10.1007/978-3-319-48006-0_3
5. Mgbemene, C., Jacobs, I., Okoani, A. and Ononiwu, N. (2022). Experimental investigation on the performance of aluminium soda can solar air heater. *Renewable Energy* 195 182-193. https://doi.org/10.1016/j.renene.2022.06.011
6. Resti, Y., Mohruni, A.S., Burlian, F., Yani, I. and Amran, A. (2017). A probability approach in cans identification. MATEC Web Conf. 101 03012. https://doi.org/10.1051/matecconf/201710103012
7. Brough, D. and Jouhara, H. (2020). The aluminium industry: A review on state-of-the-art technologies, environmental impacts and possibilities for waste heat recovery. *International Journal of Thermofluids* 1-2 100007. https://doi.org/10.1016/j.ijft.2019.100007
8. Alvarez, G., Arce, J., Lira, L. (2004). Thermal performance of an air solar collector with an absorber plate made of recyclable aluminum cans. *Solar Energy* 77 (1): 107-113. https://doi.org/10.1016/j.solener.2004.02.007
9. Ozgen, F., Esen, M. and Esen, H. (2009). Experimental investigation of thermal performance of a double-flow solar air heater having aluminium cans. *Renewable Energy* 34 (11): 2391-2398. https://doi.org/10.1016/j.renene.2009.03.029
10. Abdullah, A., Abou Al-sood, M., Omara, Z., Bek, M. and Kabeel, A. (2018). Performance evaluation of a new counter flow double pass solar air heater with turbulators. *Solar Energy* 173 398-406. https://doi.org/10.1016/j.solener.2018.07.073
11. Kishk, S.S., ElGamal, RA.. (2019). Effectiveness of recyclable aluminum cans in fabricating an efficient solar collector for drying agricultural products. *Renewable Energy* 133 307-316. https://doi.org/10.1016/j.renene.2018.10.028
12. Abdullah, A.S., Amro, M., Younes, M., Omara, Z.M. and Kabeel, AE. (2020). Experimental investigation of single pass solar air heater with reflectors and turbulators. *Alexandria Engineering Journal* 59 579-587. https://doi.org/10.1016/j.aej.2020.02.004
13. Murali, G., Reddy, K.R.K., Kumar, M.T.S., SaiManikanta, J. and Reddy, VNK. (2020). Performance of solar aluminium can air heater using sensible heat storage. *Materials Today: Proceedings* 21 169-174. https://doi.org/10.1016/j.matpr.2019.04.213
14. Khanlari, A., Tuncer, A.D., Afshari, F. and Sözen, G. (2023). Utilisation of recyclable aluminum cans as fins in a vertical solar air heating system: An experimental and numerical study. *Journal of Building Engineering* 63 105446. https://doi.org/10.1016/j.jobe.2022.105446

15. Hajizadeh Aghdam, A., Rezaei, P. and Baraheni, M. (2023). Design, fabrication, and performance assessment of a novel solar air heater based on recycled materials. *Future Technology* 2 (4): 17-23. https://doi.org/10.55670/fpll.futech.2.4.2
16. Asowata, O., Swart, J. and Pienaar, C. (2012). Optimum tilt angles for photovoltaic panels during winter months in the Vaal triangle, South Africa. *Smart Grid and Renewable Energy* 3 (02): 119. http://doi.org/10.4236/sgre.2012.32017
17. Duffie, J.A., Beckman, W.A. and Blair, N. (2020). Solar engineering of thermal processes, photovoltaics and wind. John Wiley & Sons.
18. Sales, A., Rodrigues, S.J., Mahesh, M., Ginjupalli, K., Shetty, T., Pai, U.Y., Saldanha, S., Hegde, P., Mukherjee, S., Kamath, V., Bajantri, P., Srikant, N. and Kotian, R. (2022). Effect of Different Surface Treatments on the Micro-Shear Bond Strength and Surface Characteristics of Zirconia: An In Vitro Study. *International Journal of Dentistry* (1): 1546802. https://doi.org/10.1155/2022/1546802
19. Mandpe, A., Tyagi, L., Paliya, S., Chaudhry, S., Motghare, A .and Kumar, S. (2021). Rapid-in-house composting of organic solid wastes with fly ash supplementation: Performance evaluation at thermophilic exposures. Bioresource Technology 337 125386. https://doi.org/10.1016/j.biortech.2021.125386
20. Schafers, J., Warren, C.J., Yang, J., Zhang, J., Cole, S.J., Cooper, J., Drewek, K., Kolli, B.R., McGinn, N. and Qureshi, M. (2025). Pasteurisation temperatures effectively inactivate influenza A viruses in milk. *Nature Communications* 16 (1): 1173. https://doi.org/10.1038/s41467-025-56406-8
21. Spiridonov, V., Ćurić, M. and Novkovski, N. (2025). Solar Radiation: Driving Atmospheric Change. In: Atmospheric Perspectives: Unveiling Earth's Environmental Challenges. Springer. https://doi.org/10.1007/978-3-031-86757-6_7
22. Stieglitz, R. and Platzer, W. (2024). Solar Radiation. In: Solar Thermal Energy Systems: Fundamentals, Technology, Applications. Springer.
23. Fahmi, M, Khalil, W and Shareef, A. (2020). Experimental Investigation of Double Pass Solar Air Collector for Using in Agricultural Applications. Iraqi Journal of Desert Studies 98-117.

Statements and Declarations

Funding: This study was supported by the Agricultural Research Council (ARC) and the University of KwaZulu-Natal

Competing interests: The authors have no relevant financial or non-financial interests to disclose.

Authors' Contributions: Sishosonke Caspar Nsele: Conceptualisation, study design, construction of the solar air heater, data collection, data analysis, and original draft preparation. Dr Alaika Kassim: Supervision, conceptualisation, guidance on methodology, and review and editing of the manuscript. Dr. Sipho Sibanda: Supervision, review, and critical revision of the manuscript. Prof. Tilahun Workneh: Supervision, review, critical revision of the manuscript, and guidance on data interpretation.

Data availability: The dataset generated and/or analysed during the current study is available from the corresponding authors on reasonable request.

Consent for publication: The authors are willing to permit the Journal to publish the article.

Ethics approval and consent to participate: Not applicable.